



HAL
open science

Pilot-scale direct UV-C photodegradation of pesticides in groundwater and recycled wastewater for agricultural use

S. Ferhi, Julien Vieillard, C. Garau, O. Poulter, L. Demey, R. Beaulieu, P. Penalva, V. Gobert, F. Portet-Koltalo

► To cite this version:

S. Ferhi, Julien Vieillard, C. Garau, O. Poulter, L. Demey, et al.. Pilot-scale direct UV-C photodegradation of pesticides in groundwater and recycled wastewater for agricultural use. *Journal of Environmental Chemical Engineering*, 2021, 9 (5), pp.106120. 10.1016/j.jece.2021.106120. hal-04097462

HAL Id: hal-04097462

<https://hal.science/hal-04097462>

Submitted on 22 Aug 2023

HAL is a multi-disciplinary open access archive for the deposit and dissemination of scientific research documents, whether they are published or not. The documents may come from teaching and research institutions in France or abroad, or from public or private research centers.

L'archive ouverte pluridisciplinaire **HAL**, est destinée au dépôt et à la diffusion de documents scientifiques de niveau recherche, publiés ou non, émanant des établissements d'enseignement et de recherche français ou étrangers, des laboratoires publics ou privés.



Distributed under a Creative Commons Attribution - NonCommercial 4.0 International License

1 **Pilot-scale direct UV-C photodegradation of pesticides in groundwater and recycled**
2 **wastewater for agricultural use.**

3 S. Ferhi^{1, 2}, J. Vieillard², C. Garau^{1, 2}, O. Poulthier³, L. Demey⁴, R. Beaulieu^{1,5}, P. Penalva⁶, V.
4 Gobert⁴, F. Portet-Koltalo^{2, *}

5

6 1 Seed Innovation Protection Research Environment, Comité Nord – SIPRE, Rue des
7 Champs Potez, 62217 Achicourt, France.

8 e-mails: sabrina.ferhi@yahoo.fr; charlene.garau@gmail.com

9 2 Normandie University, UNIROUEN, COBRA laboratory UMR CNRS 6014, 55 rue Saint
10 Germain, 27000 Evreux, France.

11 e-mails: florence.koltalo@univ-rouen.fr; julien.vieillard@univ-rouen.fr

12 3 CRT PRAXENS, 55 rue Saint Germain, 27000 Evreux, France

13 e-mail : contact@praxens.fr; n.picard@praxens.fr

14 4 FN3PT/inov3PT, French Federation of Seed Potato Growers, Rue des Champs Potez,
15 62217 Achicourt, France

16 e-mail: laura.demey@inov3pt.fr; virginie.gobert@inov3pt.fr

17 5 Laboratoire de Glycochimie, des Antimicrobiens et des Agroressources (LG2A) CNRS
18 UMR 7378, and Institut de Chimie de Picardie FR 3085, Université de Picardie - Jules Verne,
19 80039 Amiens, France.

20 e-mail: beaulieu.remi@yahoo.com

21 6 Normandie Sécurité Sanitaire, 55 rue Saint Germain, 27000 Evreux, France.

22 e-mail: contact@n2s.fr

23

24 *** Author to whom correspondence should be addressed:**

25 e-mail: florence.koltalo@univ-rouen.fr ; Tel.: +33-232-291-535; Fax: +33-232-291-539.

26

27 **Abstract**

28

29 Pesticides widely used for intensive agriculture may leach to groundwater and pose problems
30 to drinking water and irrigation. UV-C disinfection systems (UV-DS) for water disinfection
31 can be used also for the abatement of organic micropollutants. A pilot-scale continuous flow-
32 through UV-DS system was evaluated for its degradation efficiency of atrazine (ATR),
33 malathion (MAL) and glyphosate (GLY) from 40 L water. Groundwater used to irrigate
34 potato fields and recycled wastewater used to wash potatoes were treated without catalysts to
35 avoid any toxicity effect on potatoes. Chromatographic methods were used to quantify very
36 low pesticide levels before and after UV-C treatments ($<10 \mu\text{g L}^{-1}$), while a specific method
37 was adapted to analyse traces of GLY ($0.0008\text{-}10 \mu\text{g L}^{-1}$) in recycled wastewater containing
38 suspended particulate matter (SPM). ATR was completely eliminated from groundwater after
39 15 min photodegradation while 80% was removed from the turbid wastewater after 25 min.
40 For MAL, 70-80% was removed in 25 minutes from the groundwater. For wastewater, the
41 initial concentration was important for the performance of the photolytic process. An amount
42 of 75% of GLY was eliminated after 10 minutes irradiation at concentrations higher than
43 those found in natural groundwater. In wastewater, the UV-C treatment was less efficient
44 because GLY was mainly adsorbed to SPM which obstruct the photodegradation process.
45 Therefore, the pilot-scale UV-DS using a turbulent flow and a multiple-lamp system was
46 performant to remove quantitatively traces of pesticides from large volumes of water, by
47 direct photolytic oxidation, when the turbidity of the treated water was limited.

48

49 **Key words**

50 UV-C photolysis; recycled water; pesticides; glyphosate; pilot-scale treatment; ultra-trace
51 analysis

52

53 **Abbreviations**

54

55 AOP: Advanced oxidation processes

56 AMPA: aminomethylphosphonic acid

57 ATR: Atrazine

58 CIP: Cleaning in place

59 DEA: Desethylatrazine

60 DI: Deionized

61 DIA: Deisopropyl-atrazine

62 DOM: Dissolved organic matter

63 FLD: Fluorescence detection

64 FMOC: Fluorenylmethoxycarbonyl

65 GC-MS: Gas chromatography coupled to mass spectrometry

66 GLY: Glyphosate

67 HA: Humic acids

68 IARC: International Agency for Research on Cancer

69 LC: Liquid chromatography

70 LOD: Limit of detection

71 LOQ: Limit of quantification

72 MAL: Malathion

73 SIP: Sterilization in place

74 S/N: Signal to noise

75 SPE: Solid phase extraction

76 SPM: Suspended particulate matter

77 UV-DS: UV disinfection systems

78

79 **1. Introduction**

80 The extension of intensive agriculture worldwide has led to an increase in the use of
81 pesticides for plant and crop protection in the past decades and they have become among the
82 most frequently occurring organic pollutants in surface and groundwater [1, 2]. A majority of
83 pesticides are persistent and resist to natural degradation processes and so they remain for
84 extended periods in soils (after field applications) where they can accumulate. Some
85 pesticides may leach to groundwater and pose problems for drinking water and irrigation.
86 Because of possible adverse effects on the environment and human health caused by a
87 majority of pesticides, the European Union established a maximum permissible concentration
88 of $0.1 \mu\text{g L}^{-1}$ in drinking water for one target pesticide and a total concentration of $0.5 \mu\text{g L}^{-1}$
89 for the sum of them [3].

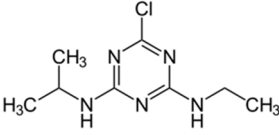
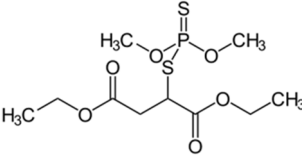
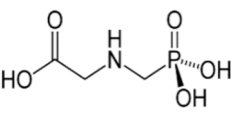
90 Each year in France, more than 5 billion m^3 of water is collected for agricultural use, of which
91 60% is used for irrigation. In potato production, 0.6 m^3 water is required to produce 1 kg of
92 potato tubers. In a context of sustainable development and to save drinking water, wastewater
93 is expected to be recycled and reused, but the presence of pesticides above regulated
94 concentrations can, as for irrigation water, pose a serious problem.

95 Atrazine (ATR) is one of the most commonly used herbicides in the world [4]. It is not
96 volatile, not very polar and not very soluble in water, and it can accumulate onto soil organic
97 matter (Table 1). Before its ban in France in 2003, the organochlorine ATR was commonly
98 used in corn and wheat cultivation, but also in potato fields. ATR and two of its degradation
99 products (desethylatrazine (DEA) and hydroxyatrazine) were among the most detected
100 substances in the French rivers between 2009 and 2013 [5]. ATR is classified in group 3 of
101 the International Agency for Research on Cancer (IARC), with an inadequate evidence for the
102 carcinogenicity in humans but a sufficient evidence in experimental animals (Table 1).

103 After 2003, ATR was largely replaced by glyphosate (GLY) in France, which is now the most
104 widely used herbicide and became (with its main transformation product
105 aminomethylphosphonic acid (AMPA)) the most measured in French rivers [6]. GLY is a
106 non-selective broad-spectrum organophosphate herbicide, not volatile, very polar and very
107 soluble into water (Table 1). However, it can also accumulate into soils through the formation
108 of complexes with soil cations, depending on soil pH [7]. In 2015, IARC classified GLY as
109 “probably carcinogenic to humans” (Group 2A) (Table 1). GLY drifts can also cause leaf
110 deformation of potato plants and can consequently lead to serious economic losses for
111 impacted producers after lot rejections. Just like GLY, malathion (MAL) is an
112 organophosphorous compound but is generally used as an insecticide. As ATR, MAL is
113 neither volatile, nor being very polar and not very soluble into water, so it can accumulate
114 onto soil organic matter (Table 1). It has been forbidden in France since 2007, but it was
115 previously used to eliminate fungi from seed potato lots. Even if it is no more a major
116 pesticide found in French rivers, it is a dangerous persistent compound, which has been
117 classified as “probably carcinogenic to humans” (Group 2A) by IARC (Table 1), as one of its
118 transformation product malaaxon.

119 Table 1: Physico-chemical and carcinogenic characteristics of the studied pesticides

120

	Atrazine	Malathion	Glyphosate
Chemical structure			
pKa	1.64	-	2.34; 5.73; 10.2
Vapour Pressure (25°C) (Pa)	3.85×10^{-5}	4.5×10^{-4}	1.31×10^{-5}
Solubility (20°C) (mg L ⁻¹)	30	145	10,500 (pH=2)
Log K _{ow}	2.5	2.8	-3.2 (pH=5-9)
K _{oc} (L kg ⁻¹)	86	151-308	81-7564
Maximal absorption wavelength (nm)	225 [8]	210 [8]	< 200 (pH=7) [9]
Carcinogenicity (IARC)	Group 3	Group 2A	Group 2A

121

122

123 As pesticides can adversely impact aquatic environment at low levels and must be analysed at
124 trace levels in groundwater as well as in drinking water, sensitive analytical methods must be
125 developed. ATR and MAL can be analysed using liquid chromatography (LC) or gas
126 chromatography coupled to mass spectrometry detection (GC-MS) but a pre-enrichment
127 procedure (using solid phase extraction (SPE) for example) is generally required to reach
128 concentrations lower than $0.1 \mu\text{g L}^{-1}$ [10-12]. GLY and AMPA are generally analysed using
129 LC coupled to MS or to fluorescence detection (FLD), but they can also be analysed using
130 GC requiring previous derivatization [13-15]. As for ATR and MAL, various preparation
131 steps must be developed before analysis (SPE, lyophilisation, large volume injections...) to
132 analyse GLY and AMPA at trace levels [16-19].

133 Ultraviolet (UV) radiation-based processes are feasible treatment solutions to eliminate or
134 drastically decrease a broad range of persistent organic pollutants such as pesticides in
135 aqueous effluents. UV-C direct photolysis has been reported to achieve better degradation of
136 persistent organic compounds than UV-A due to its higher energy [20, 21]. Photolysis
137 processes include direct photolysis of compounds that are excited by absorbing energy from
138 UV-C photons (180-280 nm) resulting in bond cleavage or rearrangement. ATR, MAL and
139 GLY can potentially absorb such energies and could be possibly degraded (Table 1). But
140 indirect photolysis can also occur when photons are absorbed by photoactive compounds
141 producing reactive oxygen species (ROS) or dissolved organic matter (DOM) in excited state
142 [22]. The application of a photocatalyst in advanced oxidation processes (AOPs) can enhance
143 the degradation of too stable or photo-inactive compounds by a significant increase of the
144 generation of ROS that oxidize and degrade them [23, 24]. UV-C disinfection systems (UV-
145 DS) can be simultaneously used for water disinfection (eliminating pathogens) [25] but also
146 for the abatement of organic micropollutants in water. The lower generation of toxic
147 byproducts during the process compared to AOPs using catalysts can be an advantage of UV-

148 DS to treat aqueous effluents in contact with food or vegetables [26]. For example, the UV-C
149 treatment of MAL in presence of TiO₂ catalyst produces more phosphate byproduct, which
150 can be toxic [27].

151 In some agricultural practices, cooperatives ensure the reception of tons of potatoes that must
152 be washed before their conditioning and delivery. Potatoes tubers are washed with natural
153 groundwater and then wastewater is intended to be continuously collected and recycled for
154 subsequent potatoes tubers cleaning, in order to save thousands cubic meters of water and to
155 develop a circular economic model. In such current process, leached persistent pesticides can
156 accumulate after few washing cycles, leading to significant exceedance of tolerated levels.
157 UV-DS can be a promising technology to eliminate leached pesticides from wastewater in
158 order to reuse it after each washing cycle. But continuous flow-through UV-DS reported
159 experiments are rare and their degradation efficiency are not well known [28]. Moreover, the
160 scaling up of photolysis or photocatalytic reactors is limited and studies are required for
161 testing large-scale photodegradation processes and determining kinetic models for a variety of
162 aqueous effluents, particularly natural water containing mixtures of persistent pollutants [29].

163 In this study, a pilot-scale disinfection process using UV-C irradiation for treating water in a
164 continuous flow-through system was evaluated for the first time for its degradation efficiency
165 of three pesticides, ATR, MAL and GLY (and some of their transformation products).
166 Groundwater used to irrigate potato fields and recycled wastewater used to wash potatoes
167 were treated. No chemical catalyst was introduced to avoid any interaction with potatoes used
168 for animal or human feed. The disappearance kinetics of the three targeted compounds were
169 established. In the case of GLY/AMPA a new SPE-HPLC-Fluorimetry analytical method had
170 to be developed to reach ultra-trace levels in water containing solid particulate matter.

171

172 **2. Material and methods**

173 **2.1 Materials**

174 2.1.1 Chemicals

175 Standards of ATR, MAL, deisopropyl-atrazine (DIA), diethyl-atrazine (DEA), malaoxon,
176 isomalathion and fluorenylmethoxycarbonyl chloride (FMOC-Cl) were obtained from Sigma
177 Aldrich (Saint Quentin Fallavier, France). GLY, AMPA, derivatized GLY-FMOC and
178 AMPA-FMOC were from Dr Ehrenstorfer GmbH (Augsburg, Germany). Deuterated labelled
179 analytical standards atrazine-d5 (ATR-d5) and malathion-d10 (MAL-d10) were from Sigma
180 Aldrich.

181 The LC grade solvents acetonitrile, dichloromethane, methanol and ethylacetate were
182 purchased from Fischer Scientific (Illkirsh, France) while octanol was from Sigma Aldrich.
183 Boric acid, sodium bicarbonate and formate ammonium were from Fisher Scientific.
184 Potassium chloride and sodium hydroxide were from Sigma Aldrich, while disodium EDTA
185 was from VWR (Strasbourg, France). Formate ammonium buffer 10 mM (pH 8) was prepared
186 by mixing 10 mL of formate ammonium 1 M and 6.19 mL of sodium hydroxide 1 M in 1 L
187 pure deionized (DI) water. Borate buffer 0.3 M (pH 8.7) was prepared by mixing 25 mL of a
188 solution of boric acid and potassium chloride (0.3 M each) with 10.7 mL of sodium hydroxide
189 0.3 M in 100 mL DI water.

190 Oxy-Anios 5 (Laboratoires ANIOS, France), the solution used to clean the UV-C pilot, was a
191 solution of peracetic acid (48 mg g⁻¹) and hydrogen peroxide (255.9 mg g⁻¹).

192

193 2.1.2 Water sampling

194 Pure DI water was supplied by a Milli-Q water system (Fisher Scientific). A large volume of
195 drilling water as well as wastewater from potato tubers cleaning was necessary to conduct the
196 pilot study. Drilled water used for irrigation of potato crops was sampled from a potato field
197 area near Evreux, Normandy France. Direct access to the drilling point was possible and

198 sampling was done with the aid of a lance. A description of the drilling point is presented in
199 Figure S1 (supplementary materials). Groundwater is commonly used for crop irrigation due
200 to its high degree of purity as a result of natural filtration through the soil. However, in recent
201 years pure groundwater has become increasingly scarce due to drought and/or otherwise,
202 contaminated by pesticide residues. Groundwater had a pH of 8.2, a mean conductivity of
203 $0.453 \pm 0.006 \text{ mS cm}^{-1}$ (n=9) and a mean turbidity of $21.6 \pm 3.0 \text{ FTU}$ (n=9). Compared with
204 typical French tap water (turbidity $\leq 2 \text{ FTU}$ and $0.180 \leq \text{conductivity} \leq 1 \text{ mS cm}^{-1}$, quality
205 reference values from 2001-1220 French decree), the collected groundwater was slightly
206 turbid and contained few ionized mineral salts.

207 Wastewater from potato tuber cleaning was sampled with a pump, which was inserted into a
208 clean settled reservoir that collects wastewater from a potato packaging company. The
209 reservoir is made up of four water pools which are inter-connected. As such, movement of the
210 wastewater from the potatoes cleaning point crosses the four water pools, with debris settling
211 in each of the pools, thus water arriving at the last pool is clearer and is intended be reused for
212 cleaning potato tubers. Apart from this pre-treatment step, there was no additional treatment
213 applied to the wastewater. As such, it is possible that all potato crop-related treatments and
214 microbial contaminants or pathogens of the potato tubers maybe leached into the reservoirs,
215 leading to an accumulation of pesticides and proliferation of pathogens. It is why the
216 SurePure TurbulatorTM device was expected to be installed after the last reservoir for an
217 additional treatment of the washing water (Figure S2). Wastewater had a pH of 7.9, a mean
218 conductivity of $0.477 \pm 0.020 \text{ mS cm}^{-1}$ (n=9) and a mean turbidity of $492 \pm 91 \text{ FTU}$ (n=9). As
219 compared with typical French tap water, the recycled water was very turbid and contained few
220 ionized mineral salts.

221 After sampling, ground- or wastewater was stored at room temperature in 10 L plastic
222 containers, previously rinsed to eliminate plastic debris and avoid any possible contamination
223 of the samples before analyses.

224 After water collection at the outlet of the disinfection setup, ground- or waste-water was
225 centrifuged at 10,000 g for 5 min to eliminate a maximum of suspended particulate matter
226 (SPM).

227

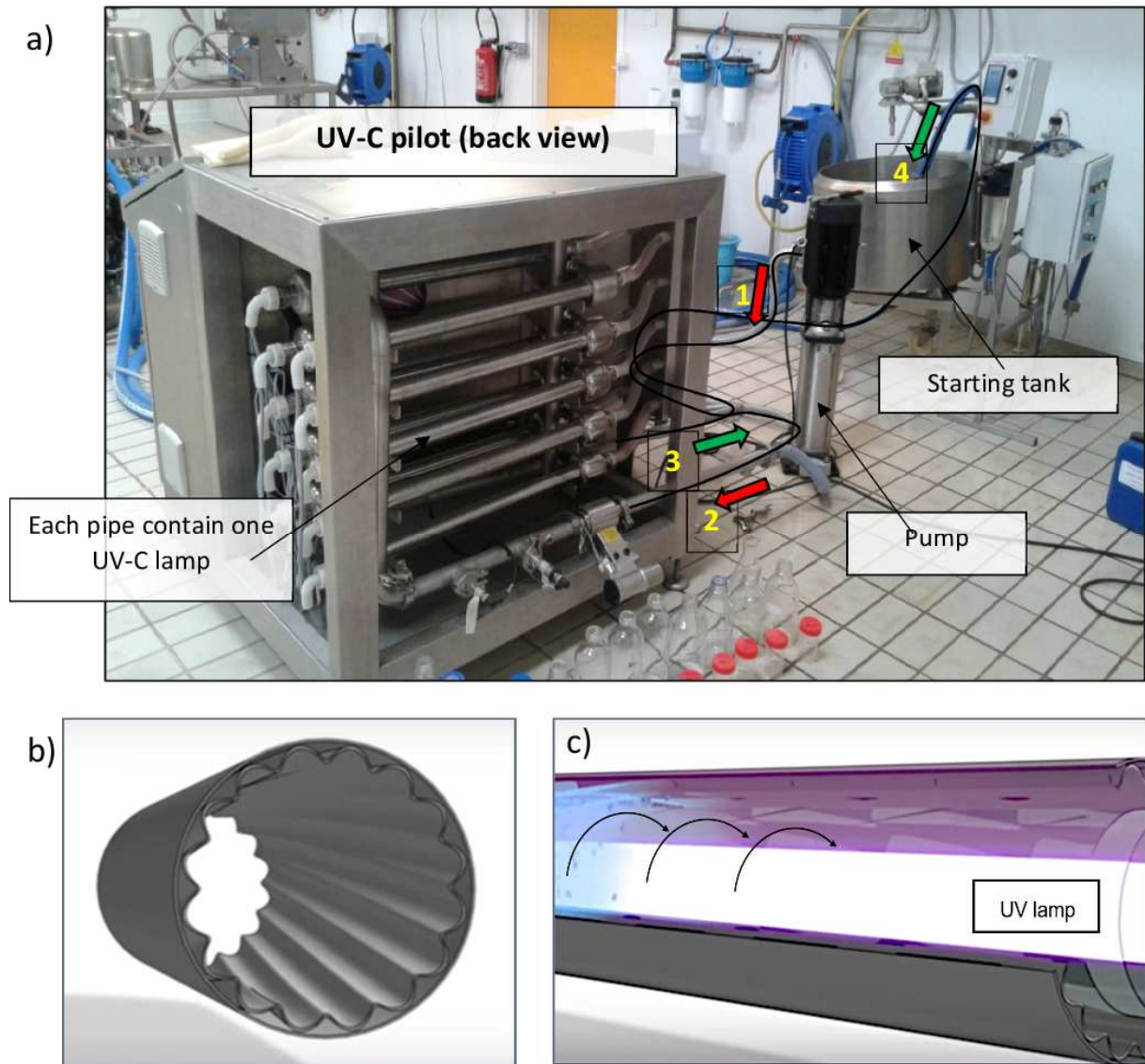
228 **2.2 Experimental disinfection setup and procedure**

229 2.2.1 Experimental setup

230 Fig. 1 shows the pilot-scale disinfection set-up (SurePure Europe). The patented SurePure
231 TurbulatorTM device exploits swirling turbulent flows and is designed for continuous flow of
232 turbid fluids, so it is well adapted for treating complex solutions such as wine, blood, milk
233 [30]. The turbulent flow and the multiple-lamp system (primarily used as germicide lamps)
234 increase the liquid exposure to UV-C, limiting biofouling, enabling greater homogeneity and
235 efficiency in purification. The disinfection pilot consists of a reservoir tank that can contain
236 100 L water, of a liquid pump (flow-rate 4500 L h⁻¹), of 10 quartz pipes of 80 cm long and 78
237 mm diameter in a series circuit, each containing one mercury lamp (254 nm wavelength) (Fig.
238 1). Each lamp is protected by a quartz sleeve and can deliver 36 W (which corresponds to 29
239 W in the UV-C range), but with 15% loss due the quartz tubing material (measured and
240 specified by the manufacturer).

241

242 Figure 1: (a) Pilot-scale disinfection UV-C pilot: “1” and “2” indicate the entrance water
243 flow, “3” and “4” indicate the outlet flow; (b) 3D-modelling of the stainless steel tube; (c) the
244 arrows indicate how the solution moves around the UV-C lamp.
245



246

247

248 2.2.2 Photolytic experiments procedure

249 *Cleaning and sterilization in place (CIP and SIP steps):*

250 This procedure aimed at preparing the installation for the reception of the water to be treated.
251 It consisted of a chemical cleaning and decontamination using Oxy-Anios 5. In the starting
252 tank, 200 mL of Oxy-Anios 5 (oxidizing agent) in 39.8 L water (0.5% mixture) was disposed.
253 This mixture flowed through the installation for 10 min with no light, passing through the
254 pump and the pipes, then returning in the starting tank in a close circuit. After 10 min, the
255 installation was entirely rinsed with 100 L of tap water to eliminate any remaining Oxy-Anios
256 5. Then the starting tank was again charged with 40 L of tap water which flowed for 10 min
257 through the machine but with lights switched on, in order to eliminate residual Oxy-Anios 5.
258 After rinsing, the water was eliminated and the machine was purged. At the end of each water
259 treatment, the CIP and SIP steps were undertaken.

260 *Treatment step:*

261 To prevent some damages of the machine, especially of the quartz tubes, the water to be
262 treated was previously filtered through sieves of 450 and 250 μm . The coarsest fractions of
263 particulate matter were eliminated. The 40 L water samples (to be treated) were charged in the
264 starting tank, then the connection between the tank and the pump was opened and the water
265 circulation was switched on. During the first 5 min, the lamps were not switched on allowing
266 the water to homogenize correctly in all the installation. As 32 seconds are required to flush
267 40 L of sample once in the tubes, 5 min was enough to reach a steady concentration after few
268 circulation cycles [25]. As a control sample, a non-treated water sub-sample was collected
269 before the UV-C lamps were switched on. After each exposure time (1, 3, 5, 10, 15 and 25
270 min), the lamps and the pump were stopped while 200 mL of sub-sample of treated water was
271 collected at the end-point of the pipes circuit. Then, the collecting point was closed and the
272 lamp and the pump were restarted again until the next collection.

273 **2.3 Analytical methods**

274 2.3.1 Sample preparation and GC-MS analysis of ATR, MAL and some transformation 275 products

276 After water centrifugation, a preconcentration step was performed on the supernatant using
277 solid phase extraction (SPE) with Oasis HLB 200 mg cartridges (Waters, Saint-Quentin-en-
278 Yvelines, France). Solid phase conditioning was done with 6 mL dichloromethane, 6 mL
279 acetonitrile followed by 6 mL DI water. The prepared water sample ($V=200$ to 1000 mL) was
280 passed through the SPE cartridge by a vacuum pump. The cartridge was finally dried by a
281 nitrogen flow (1 h). The analytes were eluted with 2×4 mL dichloromethane. An amount of
282 10 μ L octanol was added as solvent keeper and the eluate was evaporated to dryness 45 min
283 at 45°C and 200 mBar (Mivac concentrator, Genevac, Fisher Scientific). At the end, 170 μ L
284 ethyl acetate was added alongside 10 μ L of internal standards of deuterated ATR-d5 and
285 MAL-d10 (at 100 mg L^{-1} in methanol). An aliquot of 1 μ L was injected (splitless mode,
286 280°C) into a gas chromatographer GC (7890B, Agilent, Santa Clara, USA), coupled with a
287 mass spectrometer MS (7000C). Separation was performed using a 60 $\text{m}\times 0.25$ mm Zebron
288 ZB- SemiVolatiles capillary column (0.25 μm film thickness) obtained from Phenomenex,
289 with helium at 1.4 mL min^{-1} . The oven temperature was programmed to begin at 100°C (1
290 min), increased to 190°C ($30^{\circ}\text{C min}^{-1}$), then 200°C ($0.8^{\circ}\text{C min}^{-1}$), 230°C ($5^{\circ}\text{C min}^{-1}$) and
291 finally 240°C ($4^{\circ}\text{C min}^{-1}$). The MS detector operated at 70 eV. Quantification was based on
292 selected ion monitoring for better sensitivity. The linearity of the detection was in the range
293 0.1 - 8 mg L^{-1} for ATR, MAL, DEA, DIA, malaoxon, isomalathion, with $r^2>0.995$ for
294 calibration curves. Limits of detection (LOD) (signal to noise $S/N=3$) and quantification
295 (LOQ) ($S/N=10$) of these compounds were evaluated on real samples of recycled wastewater
296 ($V=1000$ mL) spiked with 2 $\mu\text{g L}^{-1}$ of ATR, MAL and some transformation products (Table
297 2). Their recoveries were in the range 75 - 106% (Table 2).

298 Table 2: Limits of detection, of quantification and recovery yields for the different pesticides
299 and some transformation products spiked in the turbid wastewater and analysed after SPE
300 concentration.

301

	LOD (ng L ⁻¹)	LOQ (ng L ⁻¹)	Recoveries (%) (n=5)
ATR	0.71	2.6	78.0±9.6
DIA	1.3	4.1	106.0±8.7
DEA	0.3	1.9	75.0±9.3
MAL	0.1	2.3	95.0±16.5
Malaoxon	0.5	2.5	98.0±13.7
Isomalathion	2.8	8.6	90.0±18.7
GLY *	0.25	0.84	58.0 (n= 3)

302 * Results obtained from spiked groundwater, only for GLY.

303

304 2.3.2. Sample preparation and LC-FLD analysis of GLY and AMPA

305 After water centrifugation and before the preconcentration step, 8 mL of EDTA 0.1 M
306 (pH=10, adjusted with NaOH 5M) was added to 200 mL of the aqueous supernatant and was
307 homogenized prior to filtration through a cellulose acetate filter (5-8 μm , Fisher Scientific)
308 under vacuum. The preconcentration step was performed using a PSOH Chromabond (500
309 mg) SPE cartridges (Macherey Nagel, Hoerdt, France). Solid phase conditioning was done
310 with 2 \times 2 mL DI water, then 2 \times 1 mL sodium bicarbonate (1 M) followed by 2 \times 2 mL DI
311 water. Then the water sample mixed with EDTA was passed through the SPE cartridge with
312 the aid of a vacuum pump. After drying the cartridge under N₂ flow, analytes were eluted with
313 2 \times 1 mL KCl 1 M.

314 For the derivatization step, 0.4 mL borate buffer 0.3 M (pH 8.7) was added to the eluate and
315 shaken for 20 s. Then 0.4 mL of FMOC-Cl (6 mM into acetonitrile) was added and the
316 mixture was shaken in darkness for 20 min. Thereafter, 3 \times 1 mL ethyl acetate were added and
317 after shaking, the lower aqueous phase was recovered and analysed using LC (Beckman Gold
318 126, Villepinte, France) coupled with a fluorimetric (FLD) detector Prostar 363 Varian
319 (Agilent). An amount of 20 μL of sample was injected into a Gemini C₁₈ column (150 \times 4.6
320 mm, d_p =5 μm) (Phenomenex), at 30°C and with a flow-rate of 1 mL min⁻¹. The mobile phase
321 was composed of solutions (A) (ammonium formate 10 mM, pH 9.5) and (B) (acetonitrile).
322 The analysis began with 15% (B) for 5 min, followed by a linear gradient to 98% (B) over 15
323 min before stabilizing at 98% (B) over 5 min. Optimal fluorescence excitation/emission
324 wavelengths were, respectively, 250/310 nm to obtain a sensitive detection. The linearity of
325 the detection was in the range 1-30 $\mu\text{g L}^{-1}$ for GLY and AMPA, with $r^2 > 0.997$ for calibration
326 curves. The LOD, LOQ and recoveries are discussed in the section 3.1 (Table 2).

327

328 **3. Results and discussion**

329 **3.1. Adaptation of the analytical methodology for the analysis of GLY at ultra-trace** 330 **levels in wastewater.**

331 GLY is often analysed at trace levels in drinking, surface water or groundwater, which do not
332 contain high amounts of SPM or DOM and rarely in raw turbid water, where it has been
333 demonstrated that GLY can be associated to particulate matter [17, 18, 31]. However, in the
334 present study, although filtration and centrifugation were performed before analysis of the
335 turbid recycled wastewater, organic colloids (DOM) and nano- or micro-particles from SPM
336 could not be fully removed. Thus, there was a requirement for the development of new
337 strategies in the sample preparation to analyse GLY at ultra-trace levels in turbid water. It was
338 particularly critical to quantify GLY at concentrations in the $\mu\text{g L}^{-1}$ range as direct
339 photodegradation processes in these low concentration ranges, encountered in environmental
340 water effluents, are not well known.

341 As GLY and AMPA were detected through a fluorimetric detector, allowing higher sensitivity
342 than UV or MS detectors, they were derivatized using an excess of FMOC-Cl, because it can
343 also react with other amines or amino acids which may be present in recycled water. FMOC-
344 Cl was prepared into acetonitrile to obtain better derivatization yields [32]. It is known that
345 the reaction must be done in alkaline conditions and that derivatization yields increase when
346 pH increase from 7.0 to 9.1, but here, a pH=8.7 was selected to avoid high hydrolysis of
347 FMOC-Cl into FMOC-OH at more alkaline pH [33]. As GLY and AMPA were obtained after
348 concentration of 200 mL water in 2 mL aqueous solutions containing concentrated KCl,
349 several volumes (300-600 μL) and concentrations (0.125-0.3 M) of FMOC-Cl were tested.
350 Even if higher amounts of FMOC-Cl favor the derivatization process, a medium volume (400
351 μL) of the highest concentrated solution was selected to avoid sample dilution. At last, the
352 best reaction time was determined allowing the formation of derivatized analytes without the

353 formation of secondary by-products. The reaction time was tested between 0-24 h [34, 35].
354 No significant difference on derivatization yields was observed after 20 min reaction ($p > 0.05$,
355 Student test, $n=3$) and after 1h, higher amounts of secondary by-products could be observed.
356 Therefore, 20 min derivatization was selected, obtaining mean derivatized glyphosate (GLY-
357 FMOC) yields of $100.8 \pm 9.7\%$ ($n=3$). Using DI water spiked with GLY and AMPA, the limit
358 of detection (LOD) ($S/N=3$) and of quantification (LOQ) ($S/N=10$) using LC-FLD after
359 derivatization were $0.013 \mu\text{g L}^{-1}$ and $0.040 \mu\text{g L}^{-1}$, respectively, for GLY-FMOC and $0.09 \mu\text{g}$
360 L^{-1} and $0.30 \mu\text{g L}^{-1}$, respectively, for AMPA-FMOC. A review on analytical methods used for
361 GLY/AMPA analyses in water using LC-FLD mentioned current LODs between 0.01 - $0.1 \mu\text{g}$
362 L^{-1} for both chemicals [36]. GLY had to be quantified into water at levels as low as $0.1 \mu\text{g L}^{-1}$,
363 so the attained LOQ could be considered satisfactory.

364 GLY spiked in turbid water can be lost, due to various sorption phenomena on solid materials.
365 Therefore, a concentration process through SPE, allowing a concentration factor of 100, was
366 developed to accurately determine ultra-traces of GLY. Derivatized GLY-FMOC and AMPA-
367 FMOC are anionic species in a large alkaline pH range, so various anion exchange SPE
368 cartridges were tested, such as Chromabond PSOH (strong anion exchanger in the OH^- form),
369 Chromabond NH_2 (weak anion exchanger with aminopropyl bonded material) and Oasis
370 MAX (containing a mixed-mode polymeric sorbent with quaternary ammonium groups).
371 Various eluting solvents were tested to desorb GLY from the SPE cartridges. With Oasis
372 MAX, aqueous solutions containing HCl (0.5 M) or sodium citrate (0.6 M) were tested, and
373 low or inconsistent recoveries ($2 \pm 2\%$ and $140 \pm 24\%$ ($n=3$ replicates), respectively) for GLY-
374 FMOC were obtained. The HCl acid was not a good eluting solvent for the further
375 derivatization step whereas sodium citrate yielded a more favorable alkaline $\text{pH}=8$. With
376 Chromabond NH_2 , aqueous solutions containing sodium citrate (0.6 M) and a phosphate
377 buffer (0.1 M, $\text{pH}=8$) gave $43 \pm 9\%$ and $108 \pm 5\%$ recoveries, respectively ($n=3$). Unfortunately,

378 the chromatographic resolution of AMPA-FMOC was deteriorated when phosphate buffer
379 was used. With Chromabond PSOH, an aqueous phase containing KCl (1 M) was used as
380 eluting solvent and gave a mean recovery of $102\pm 6\%$ ($n=3$). This latter combination for the
381 SPE step was chosen rather than the combination involving Oasis MAX/sodium citrate
382 because the relative standard deviation was lower. The reproducibility of the recovery yields
383 for quantifying GLY at very low levels in spiked DI water after SPE, evaluated on 3 tests on
384 different days, were $91.9\pm 20.4\%$ and $98.7\pm 8.7\%$ for GLY spiked at $0.1 \mu\text{g L}^{-1}$ and $0.6 \mu\text{g L}^{-1}$,
385 respectively.

386 As previously mentioned, quantifying GLY in drilling or recycled wastewater appeared not so
387 easy, as they contain more or less SPM/DOM which required an elimination before LC
388 analysis. Several membrane filters were tested, with cellulose acetate, nylon or nitrocellulose
389 materials which demonstrated 11%, 24% and 45% GLY loss, respectively. As such as, the
390 filter had to be carefully chosen to accurately quantify GLY in raw water containing particles,
391 and cellulose acetate material seemed appropriate. Moreover, even if ground- and wastewater
392 were centrifuged after their collection at the outlet of the disinfection setup in order to
393 eliminate SPM, mineral or organic colloids, they could not be totally eliminated. Mineral
394 colloids could contain iron or aluminium oxides that can sorb GLY [37]. Also, it has been
395 demonstrated that metal cations could interfere on the GLY and AMPA derivatization [17,
396 38]. Therefore, EDTA was introduced after centrifugation to precipitate mineral colloids and
397 associated bivalent metallic species in order to eliminate them with further filtration. In the
398 best analytical conditions, GLY spiked at $10 \mu\text{g L}^{-1}$ into groundwater and placed into the
399 disinfection pilot without irradiation, was quantified with 58% recovery (Table 2). The 42%
400 loss could be attributed to the sorption of GLY onto SPM/colloids (which were eliminated
401 through centrifugation, precipitation and filtration before analysis), but also to the sorption
402 onto the surface of the inox and quartz material of the pilot.

403 Concerning wastewater which was highly turbid and contained much more SPM, initial
404 concentrations of GLY were not negligible. From one collected in October 2017 and another
405 collected in March 2018, mean concentrations of $4.1 \pm 3.2 \mu\text{g L}^{-1}$ (n=5) and $2.6 \pm 0.9 \mu\text{g L}^{-1}$
406 (n=6), respectively, were measured. The main transformation product AMPA could not be
407 detected in wastewater. In comparison, GLY was initially found in groundwater at $0.3 \pm 0.2 \mu\text{g}$
408 L^{-1} (n=3) which is significantly lower ($p < 0.05$, Student test). Then GLY was spiked at $10 \mu\text{g}$
409 L^{-1} into wastewater and placed into the disinfection pilot without irradiation: it was quantified
410 with only 19% recovery. Compared with the results from groundwater, it is clear that an
411 important quantity was sorbed onto the pilot surfaces and coatings, but also on the high
412 amount of SPM/colloids and so could not be quantified in the dissolved aqueous fraction.
413 Considering the moderate GLY losses related to the presence of SPM/DOM into
414 groundwater, procedural LODs and LOQ using SPE and LC-FLD could be measured only
415 from spiked groundwater and were 0.84 ng L^{-1} and 0.25 ng L^{-1} , respectively (Table 2). Thus,
416 the very low LOQ values obtained for ATR, MAL and GLY (Table 2) allowed for the
417 quantification of those pesticides at ultra-trace levels into water of various turbidity, even
418 after their degradation following UV-C treatment.

419

420 **3.2. Degradation of pesticides using the pilot-scale disinfection process**

421 3.2.1. Energy of UV-C exposure per liter of treated water

422 The transmitted UV-C energy (or its power $P_{\text{transmitted}}$ in J s^{-1}) to the aqueous fluid through the
423 quartz tubing could be calculated using equation (1), knowing the power of each UV lamp
424 ($P_{\text{UV lamp}}$):

$$425 P_{\text{transmitted}} = (P_{\text{UV lamp}} \times \%_{\text{Loss}}) \times \text{number of lamps} = (29 \times 0.85) \times 10 = 246.5 \text{ J s}^{-1} \quad (1)$$

426 The time (t_{pass} in s) needed for the passage of the volume of water to be treated in the machine
427 could be calculated using equation (2):

428 $t_{\text{pass}} = \frac{(V_T \times 3600)}{4500} = \frac{(40 \times 3600)}{4500} = 32 \text{ s}$ (2)

429 Where V_T was the volume of water to treat (40 L) and $V=4500$ L was the total volume of
 430 water which could be delivered by the pump in 1 h.

431 The energy applied to the volume of water to treat (E_{pass} in J L^{-1}) in one passage could be
 432 calculated using equation (3):

433 $E_{\text{pass}} = \frac{(t_{\text{pass}} \times P_{\text{transmitted}})}{V_T} = \frac{(32 \times 246.5)}{40} = 197.2 \text{ J L}^{-1}$ (3)

434 We could then calculate the total energy of UV-C exposure (E_{exposure} in J L^{-1} or kJ m^{-3})
 435 (corresponding to the fluence) for each treatment time using equation (4):

436 $E_{\text{exposure}} = \frac{\text{time} \times E_{\text{pass}}}{t_{\text{pass}}}$ (4)

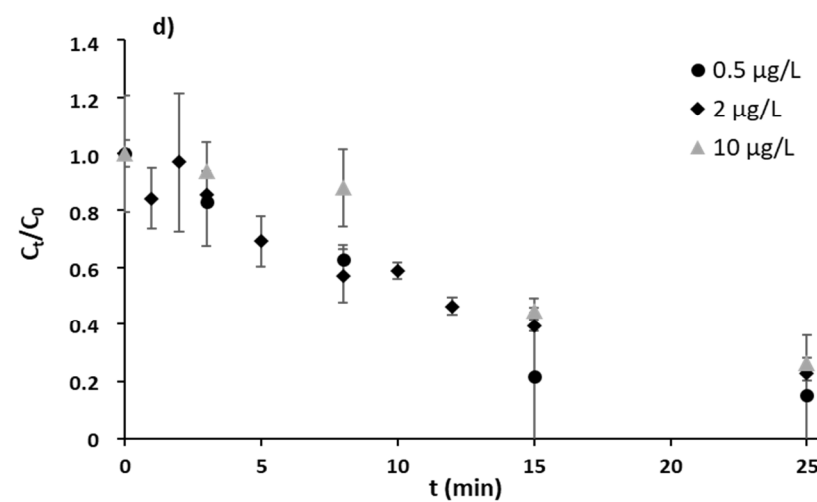
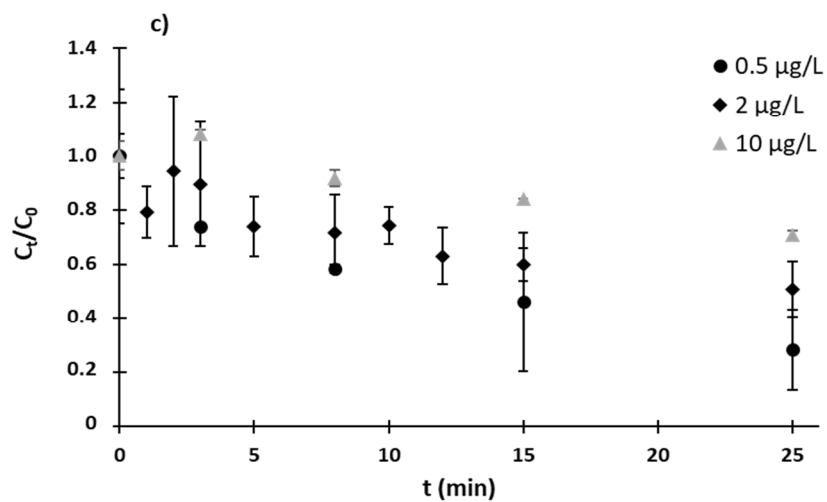
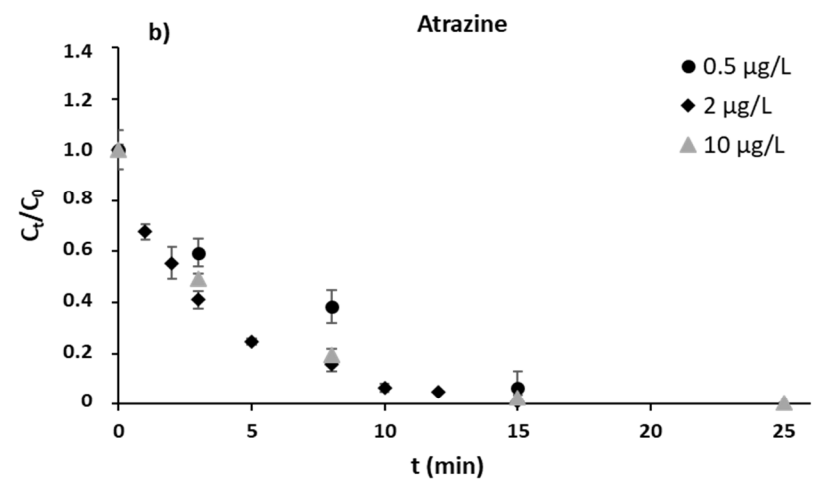
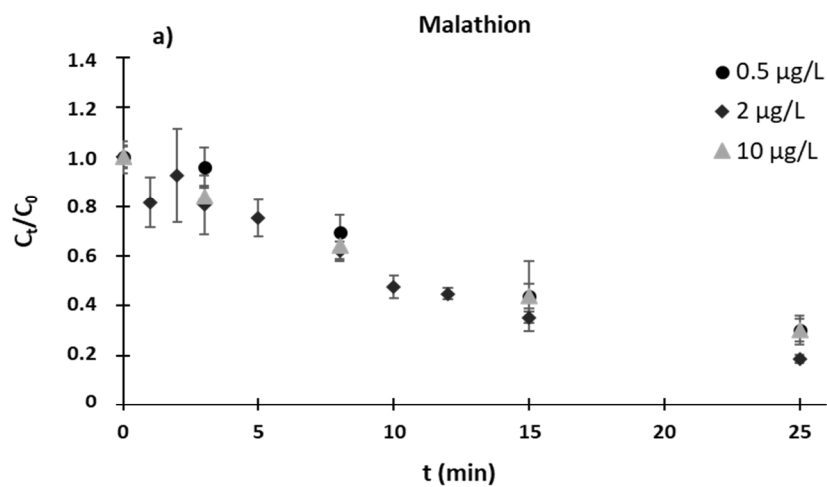
437 Where time is the treatment time (in min). Thus, the fluence could be calculated using a
 438 simple equation (5): $E_{\text{exposure}} = 369.75 \times \text{time}$ (5)

439

440 3.2.2 Dissipation of pesticides

441 *Dissipation of atrazine and malathion*

442 The kinetic curves of ATR and MAL degradation were compared according to the water
 443 treated. The measured relative concentrations (C_t/C_0) are shown as a function of the
 444 irradiation time on Fig. 2. The mean values of C_t/C_0 were obtained through duplicate
 445 experiments for a particular concentration of spiked pesticide, carried out on two different
 446 days and using two different 40 L water sample cans, which explains the variability of the
 447 results. As illustrated on equation (5), the longer the residence time into the UV-DS tubes, the
 448 higher the energy delivered from the UV-C lamps. Both MAL and ATR were quantitatively
 449 photodegraded by UV-C irradiation but a limit appeared after a few dozen minutes.



450

451 Figure 2: Plots of C_t/C_0 versus photoreaction time for MAL and ATR in groundwater (a, b) and wastewater (c, d). C_0 is the initial concentration

452 measured without irradiation ($t=0$) and C_t is the measured concentration after t (min) irradiation ($n=2$ experiments).

453 MAL and ATR could be dissipated through direct photolysis, but also through oxidation
454 reaction with ROS. Indeed, in the case of UV-C irradiation, the water molecules can
455 decompose in photoactive hydroxyl radicals that absorb the energy of irradiation [39]. The
456 yield of this reactive intermediate can reach 0.280 μmol per J of absorbed radiation energy
457 [40]. In view of eq. (5), it was possible that 1760 $\mu\text{g L}^{-1}$ could be generated per min
458 irradiation in the pilot, which is significantly above the concentrations of the dissolved
459 pesticides to remove. Moreover, other oxidants such as superoxide radical or singlet oxygen
460 could be generated: the big section of the turbulator device could help to oxygenize the
461 aqueous solution during the process and promote these ROS formation [38].

462 More than 80% ATR could be eliminated in less than 25 minutes irradiation (corresponding to
463 a fluence of 9244 kJ m^{-3} , eq. (5)) irrespective of the quality of water treated and for all the
464 tested concentrations, from 0.5 to 10 $\mu\text{g L}^{-1}$ (Fig. 2b and 2d). Only 15 minutes were necessary
465 to completely eliminate ATR from the less turbid groundwater (fluence = 5546 kJ m^{-3}) (Fig.
466 2.b). For wastewater the dissipation was limited to 80%. The larger amount of interfering
467 compounds probably interacted with the ROS, limiting the efficiency of the oxidation reaction
468 in the liquid phase. Also, the persistence of residual ATR which could not be eliminated after
469 25 min irradiation was possibly due to their sorption onto SPM, where they were not
470 accessible to direct irradiation.

471 It has been reported that DEA, DIA and 2-hydroxyatrazine are the main transformation
472 products obtained by photolysis of ATR [41, 42]. These transformation products are obtained
473 by excitation of the triazine, the dechlorination and the insertion of the hydroxyl radical
474 generated by the water photolysis. As discussed, the GC-MS method was adapted to analyse
475 ultra-traces of ATR and some of its current transformation products. The analysis of
476 groundwater and wastewater before UV-C treatment demonstrated that ATR was not
477 detectable ($<0.00071 \mu\text{g L}^{-1}$), contrary to some of its transformation products. DEA was

478 detected ($<0.002 \mu\text{g L}^{-1}$), and DIA could be quantified at $0.15\pm 0.04 \mu\text{g L}^{-1}$ ($n=4$) and
479 $0.90\pm 0.20 \mu\text{g L}^{-1}$ ($n=12$) in ground- and wastewater, respectively. Such contamination of
480 natural water by ATR metabolites, produced from the metabolic activity of bacteria, has
481 already been reported by Moreira *et al* [42]. After all the UV-C treatments, even the longer
482 ones, DEA and DIA levels were not significantly changed in treated water compared with
483 their initial concentrations. It is possible that the hydroxylation of the chlorinated carbon of
484 ATR increased the stability of the chemical structure of these compounds [42]. Thus, DEA
485 and DIA are difficult to remove by photolysis and it contributes to their prevalence and so to
486 their wide detection in various water environments, even groundwater, and for decades after
487 the phasing out of the parent molecule [43]. Also, Khan *et al.* [44] demonstrated that the
488 degradation rate of DEA and DIA increased with the increase in their initial concentration
489 when they were submitted to UV-C irradiation (254 nm). Therefore, their very low initial
490 concentrations in ground- or wastewater might also explain why no DEA or DIA
491 concentration change could be measured during the exposure to UV-C irradiation.

492 For MAL, the UV-C degradation was limited to 50-80% depending on water quality, for
493 concentrations ranging from 0.5 to $10 \mu\text{g L}^{-1}$ and after 25 min treatment (corresponding to a
494 fluence of 9244 kJ m^{-3}) (Fig. 2a and 2c). It has been reported that three oxidation by-products
495 could be generated during photolysis [45]. The degradation of MAL could be initiated by the
496 cleavage of the P-S bond to obtain the diethyl-2-mercaptosuccinate, and then the mercapto
497 group was substituted by an hydroxyl group with the help of hydroxyl radicals, to obtain the
498 diethyl malate and finally, the internal hydroxyl group could react with an hydrogen to give
499 diethyl maleate [27]. The GC-MS analysis confirmed that malaoxon and isomalathion were
500 not present, even at ultra-trace levels in water, before and after UV-C treatment, possibly
501 because the P-S bond was rapidly cleaved by photolysis.

502 The results presented in Fig. 2 indicates that the degradation was more efficient in
503 groundwater than in wastewater for both ATR and MAL. We could emphasize that SPM
504 present in the unclear wastewater limits the interaction with photons involved in the
505 photolysis and sorption protects pesticides from photolysis by competitive light attenuation
506 [46]. Moreover, the largest amount of interfering compounds (DOM and inorganic ions) in
507 wastewater should compete with ATR and MAL for photochemical reactions with ROS.
508 Particularly, humic substances can reduce the pesticide photodegradation by a strong
509 quenching effect and it can also quickly react with ROS [46, 47].

510 In both the tested water, ATR was more sensitive to UV-C degradation than MAL. Residual
511 concentrations remaining in the solution after 25 min irradiation were always greater for
512 MAL than for ATR. ATR presents a maximum absorption between 220-230 nm, so with a
513 sensitization effect more favorable than for MAL, which presents a maximum absorption
514 wavelength at the limit of the UV-C region (Table 1) [8, 41].

515 In order to better understand the photodegradation process, the kinetic of degradation was
516 evaluated for both ATR and MAL. The pseudo-first order kinetic modeling was applied in
517 waste- and groundwater according to equation (6):

$$518 \quad \ln\left(\frac{C_t}{C_0}\right) = -k t \quad (6)$$

519 where C_0 and C_t represent the concentration at time 0 and t , respectively, and k (min^{-1}) is the
520 pseudo-first order rate constant.

521 The values of the rate constants k and the coefficients of determination (r^2) corresponding to
522 the mathematical modeling (eq. 6) are summarized in Table 3. The pseudo-first order model
523 fitted well with the experimental values for ATR and MAL and it was relevant for the
524 different concentrations tested and whatever the water quality. Fig. 3 shows the plot obtained
525 from equation (6) which is in accordance with the mean experimental values (obtained from
526 duplicates).

527 Table 3: Pseudo-first order kinetic parameters for the photodegradation of MAL and ATR in
 528 ground- and wastewater.

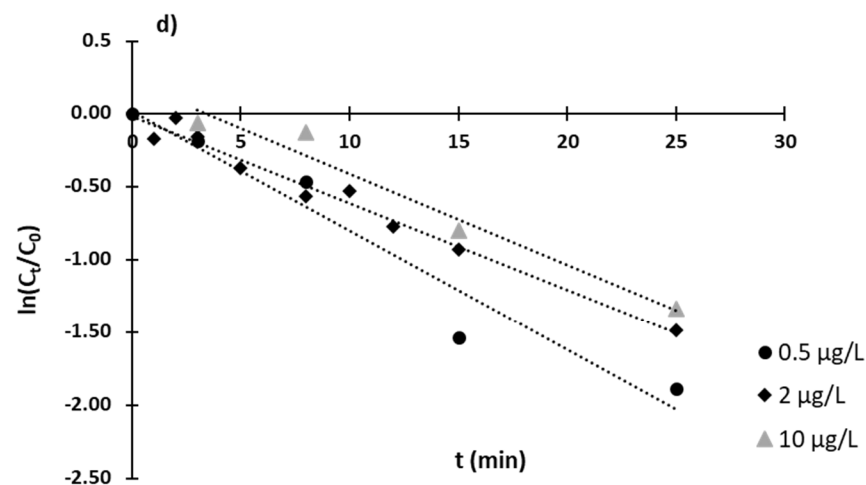
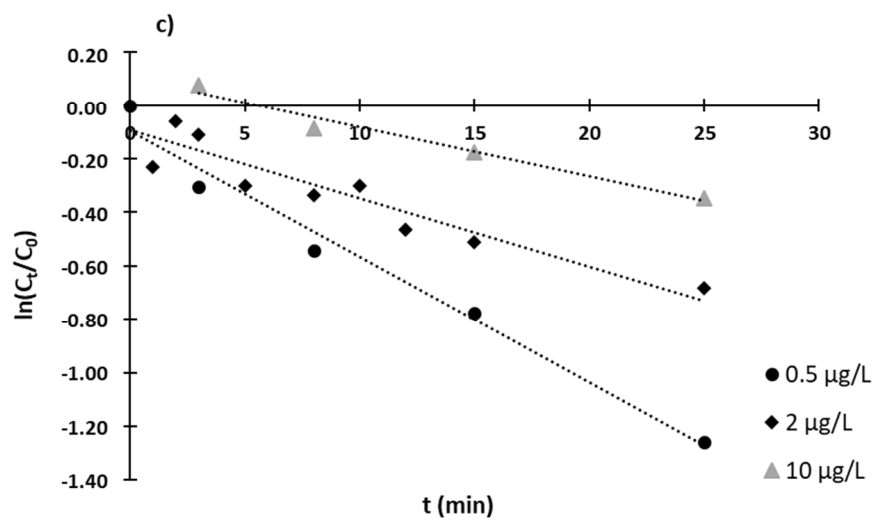
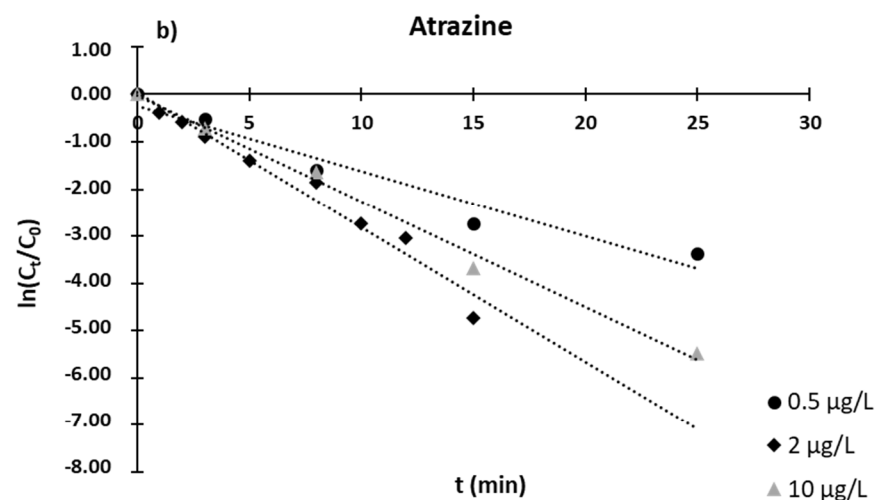
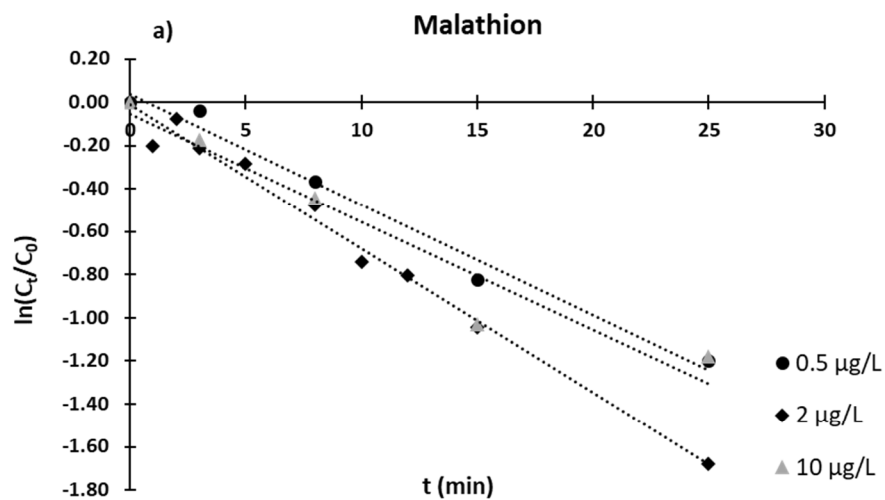
529

		Groundwater			Wastewater		
		k (min ⁻¹)	t _{1/2} (min)	r ²	k (min ⁻¹)	t _{1/2} (min)	r ²
Atrazine	0.5 µg L ⁻¹	0.1852	3.7	0.996	0.0817	8.5	0.945
	2 µg L ⁻¹	0.2847	2.4	0.970	0.0594	11.7	0.980
	10 µg L ⁻¹	0.2237	3.1	0.993	0.0622	11.9	0.964
Malathion	0.5 µg L ⁻¹	0.0512	13.5	0.980	0.0471	14.7	0.980
	2 µg L ⁻¹	0.0669	10.4	0.990	0.0257	27.0	0.870
	10 µg L ⁻¹	0.0456	15.2	0.992	0.0183	37.9	0.970

530

531

532 Figure 3: Plots of $\ln(C_t/C_0)$ versus photoirradiation time for MAL and ATR in groundwater (a, b) and wastewater (c, d).



533
534

535 Although the kinetics of the photochemical reactions can be complex because of the number
536 of steps and the reactive species involved, the OH radical is usually regarded as the sole and
537 rate limiting reactive species [46], which explains why the pseudo-first order kinetic could
538 properly model the photodegradation kinetic. According to first-order kinetics, the time
539 required for dissipating 50% of the initial concentration ($t_{1/2}$) of MAL or ATR could be
540 calculated by the equation (7):

$$541 \quad t_{1/2} = \frac{\ln 2}{k} \quad (7)$$

542 The values of $t_{1/2}$ are given in Table 3. It shows that the first stage of ATR dissipation (for
543 degrading at least one half of the molecules) was always faster than that of MAL.

544 In groundwater, the photodegradation process was less sensitive to the initial concentration of
545 ATR or MAL than in wastewater, in the range 0.5-10 $\mu\text{g L}^{-1}$. The constant rates k were only
546 slightly higher at 2 $\mu\text{g L}^{-1}$ than at 0.5 or 10 $\mu\text{g L}^{-1}$ for both the molecules in groundwater. So
547 the fluence corresponding to the dissipation of 50% of these pesticides in groundwater was
548 between 887 and 1368 kJ per m^3 of water for ATR and between 3845 and 5620 kJ per m^3 for
549 MAL, in the 0.5-10 $\mu\text{g L}^{-1}$ concentrations range. It is important to note here that continuous
550 flow-through reactor studies for organic contaminants removal by UV-C photolysis are rare at
551 the pilot scale, and that the results obtained for these pesticides are promising not only for the
552 removal capacity but also for the energy expenditure [23]. For comparison, direct UV-C
553 photolysis of a persistent pharmaceutical compound in drinking water showed degradation
554 less than 6% at 15 min, in a bench-scale continuous flow-through reactor, corresponding to a
555 fluence of 5000 kJ m^{-3} [28].

556 For wastewater, the photodegradation of ATR and MAL was significantly slower than for
557 groundwater. The time required to dissipate 50% of ATR was between 2.3 to 4.9 time longer
558 in wastewater and between 2.6 to 6 times longer for MAL (Table 3). The exception was for
559 MAL at 0.5 $\mu\text{g L}^{-1}$ whose $t_{1/2}$ was quite the same for the two water qualities. So at the lowest

560 MAL concentration, the amount of ROS seemed to be sufficient to react with MAL even in
561 the turbid water, but at MAL concentrations $> 2 \mu\text{g L}^{-1}$, $t_{1/2}$ increased drastically in wastewater
562 which shows that generated active species were no longer sufficient (Table 3). The fluence
563 corresponding to the dissipation of 50% ATR was between 3143 and 4400 kJ m^{-3} of
564 wastewater and increased from 5435 to 14014 kJ m^{-3} of wastewater for MAL, depending on
565 its initial concentration. Once again, the results obtained with the SurePure device are
566 promising, even for a very turbid water. For comparison, the removal of ten pesticides (of
567 which ATR) from leaching water containing DOM at pilot plant scale, using solar irradiation
568 (UV-A to UV-C), was less than 20% after 60 min [39].

569

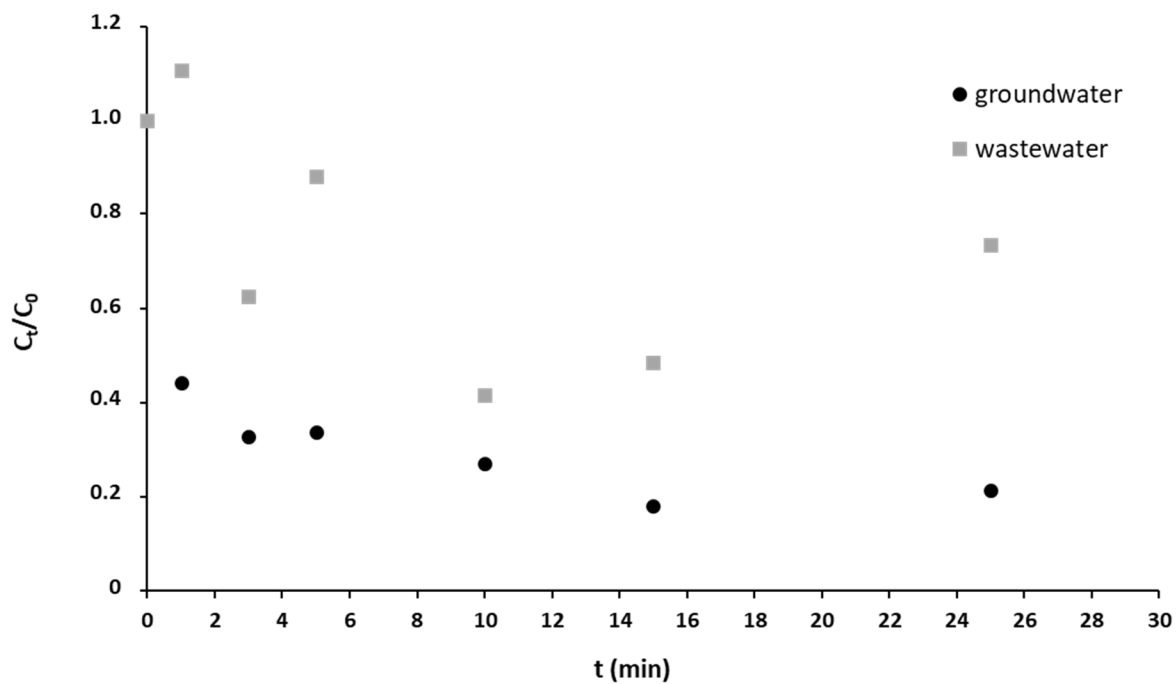
570 *Dissipation of Glyphosate*

571 The photolytic dissipation of GLY was investigated for 30 minutes (Fig. 4). Some authors
572 noted that no sign of direct photolysis was observed using UV-C irradiation for GLY at 50 mg
573 L^{-1} in pure water, which was justified by the absorption spectrum of GLY which is at the limit
574 of the UV-C region [48]. However, the sample pH is important to take into account.
575 McConnell *et al.* (1993) demonstrated that the absorption spectra of GLY could shift to
576 higher values with a pH increase. Thus, the wavelength of the maximum absorption could
577 shift to 214 nm for pHs higher than 7.0 [49]. In our case, treated waters were alkaline (7.9-
578 8.2) which could explain a part of the GLY photosensitivity.

579

580 Figure 4: Dissipation of free GLY (initial spiking: $10 \mu\text{g L}^{-1}$) in groundwater (n=3 tests) and
581 wastewater (n=1 test) after UV-C irradiation (measured in the dissolved aqueous fraction
582 from t=0).

583



584

585

586 As already mentioned (section 3.1), the direct photolysis of GLY in the very low
587 concentration ranges, found in environmental water ($\mu\text{g L}^{-1}$), is not well known, as
588 photodegradation of GLY is more often studied using spiked GLY in the mg L^{-1} range and is
589 usually assisted by photocatalysts in AOPs [50]. Here, the dissipation of GLY (spiked at 10
590 $\mu\text{g L}^{-1}$) seemed very fast in groundwater because only one minute of treatment was enough to
591 remove 57% of GLY (fluence = 370 kJ m^{-3}) (Fig. 4). It is important to note that the reported
592 C_t/C_0 values were calculated from the initial C_0 concentration measured in the dissolved
593 aqueous fraction at t_0 , just before the irradiation began, so taking into account the GLY losses
594 due to sorption (approximately 42% GLY was sorbed at t_0 (section 3.1) and could not be
595 measured in the dissolved fraction). The dissipation of free GLY was more than 75% after 10
596 minutes of irradiation, corresponding to a fluence of 3698 J m^{-3} of treated groundwater (eq.
597 (5)).

598 This fast and efficient dissipation of free GLY at low concentration ($< 10 \mu\text{g L}^{-1}$) could not be
599 fully explained by direct photolysis, but mainly by reactions with ROS such as hydroxyl or
600 superoxide radicals, for instance, and also possibly by the presence of trace of metals and
601 humic acids (HA) in groundwater. Groundwater may contain a small fraction of soluble
602 organic colloids (DOM) composed of HA complexed to iron, manganese or aluminum,
603 coming from soil lixiviation. The various aromatic compounds of HA, as polyphenols or
604 organic acids, can form charge transfer complexes with some herbicides, further sensitising
605 them for the photodegradation [51]. Also, it is known that inorganic Fe or Mn elements can
606 act as catalysts for GLY degradation by oxidation in photodegradation or electro-Fenton like
607 processes [52, 53]. In particular, HA and Fe^{3+} complexes can sensitize aquatic
608 photodegradation of GLY, with HA interacting with Fe^{3+} to produce more hydroxyl radicals,
609 causing the C-N and C-P bonds cleavage to form phosphate [53]. It should be noted here that
610 AMPA apparition could not be measured during the exposure of GLY to UV-C.

611 It must be underlined that the results obtained for GLY removal with the SurePure device are
612 very encouraging. According to the review from Diez *et al.* (2019), there was just few
613 publications on agrochemicals degradation by UV-C light at the pilot scale without catalyst
614 [23]. The cited authors reached a degradation of 30% in 100 minutes for a pesticide and 5% in
615 100 minutes for a fungicide for 19 L of treated water, demonstrating that 75% GLY removal
616 after 10 min irradiation, obtained in this work, is promising. Moreover, it is important to note
617 that these cited works were investigated in pure water and not in groundwater (or wastewater)
618 like in this study. At last, experiments on GLY using UV-C irradiation at the pilot scale are
619 even more rare and Jönsson *et al.* mentioned that the removal of GLY, spiked in drinking
620 water at $3 \mu\text{g L}^{-1}$, was not exceeding 36% after 7 days of treatment with UV-C irradiation in a
621 flow through system [54].

622 For wastewater, the performance of photolysis was also interesting with more than 50% of the
623 initial concentration of free GLY removed from the water after 10 minutes exposure and a
624 fluence of 3698 kJ m^{-3} (Fig. 4). However, after 10 minutes, the concentration of soluble GLY
625 increased in the pilot, indicating that a part of GLY was again released in the aqueous phase.
626 Compared with groundwater, an important part of GLY was sorbed to the pilot surfaces
627 (stainless steel and quartz tubes) as well as to the high amount of SPM. Approximately 80%
628 GLY was sorbed to all the solid surfaces (known initial spiked amounts were compared with
629 those measured after equilibrium of wastewater into the pilot and the water collected at t_0 , just
630 before the irradiation began). It has been reported that GLY and AMPA were more frequently
631 found associated with SPM than in the soluble phase despite their high solubility, with
632 partition coefficients in the range of $81\text{-}7564 \text{ L kg}^{-1}$ which is significantly higher than those of
633 ATR and MAL (Table 1) [9, 31, 55]. Therefore, in the case of the turbid wastewater, a
634 photodegradation of the soluble GLY fraction may occur rapidly, although SPM limit the
635 interaction with photons and the generation of hydroxyl radicals with the aid of HA from

636 DOM. However, particulate matter tended to release sorbed GLY, possibly at each water
637 cycle and because the solid/liquid partition was continuously modified in this dynamic
638 system. Unfortunately, GLY disappearance was lower than GLY release. It means that UV-C
639 irradiation must be significantly longer than 30 min to eliminate all the dissolved GLY
640 molecules from the turbid water.

641

642 **Conclusions**

643 This study investigated the degradation of ATR, MAL and GLY pesticides by direct UV-C
644 photolysis in order to develop a circular economic model to clean water used in agriculture.
645 The direct photolysis, applied in a continuous flow-through system which could treat 40 L
646 water, was investigated on natural spiked ground- and wastewater. For diluted ($0.5 \mu\text{g L}^{-1}$)
647 and more concentrated ($10 \mu\text{g L}^{-1}$) solutions, ATR was completely eliminated after 15
648 minutes from groundwater while 80% was removed from the more turbid wastewater after 25
649 minutes treatment. The GC-MS analysis demonstrated that ATR was not quantitatively
650 converted to DIA or DIE and that trace levels of these transformation products were not
651 eliminated by UV-C treatment in both water samples. For MAL, 70 to 80% (as a function of
652 the initial concentration) was removed in 25 minutes from the groundwater by photolytic
653 oxidation. For wastewater, the initial concentration of MAL was important on the
654 performance of the photolytic process. The dissipation of GLY at concentrations ($10 \mu\text{g L}^{-1}$)
655 higher than those found in natural groundwater was promising because it was quantitatively
656 eliminated after 10 minutes of irradiation (>75%), possibly with the aid of HA. In wastewater
657 containing high amount of SPM, the UV-C treatment was less efficient because GLY was
658 mainly adsorbed to particles which obstruct the photodegradation process. It seems that only
659 dissolved GLY could be photodegraded at low concentration and the continuous release of
660 GLY from particles in the dynamic UV-DS system was an obstacle to its rapid quantitative
661 elimination. This study therefore, demonstrated that the UV-C treatment applied to large

662 volumes of water, using a turbulent flow and the multiple-lamp system, was effective to
663 rapidly and quantitatively remove some herbicides and pesticides by direct photolytic
664 oxidation, without added catalysts, when the turbidity of the treated water is limited.

665 As transformation products can sometimes be more toxic than parent pesticides, the ability of
666 the UV-C treatment to remove quantitatively problematic pesticides in water will need, in the
667 future, to be supported by toxicity assays and researches on potential ecological effects.

668

669

670 **Acknowledgements**

671 The authors acknowledge the Labex SYNORG (ANR-11-LABX-0029), the Région
672 Normandie (CRUNCH and Sésa network) and ERDF (Cos-Sésa) for support.

673

674 **References**

- 675 [1] E. Villanneau, N.P.A. Saby, D. Arrouays, C.C. Jolivet, L. Boulonne, G. Caria, E. Barriuso, A. Bispo, O.
676 Briand, Spatial distribution of lindane in topsoil of Northern France, *Chemosphere*, 77 (2009) 1249-
677 1255. <https://doi.org/10.1016/j.chemosphere.2009.08.060>
- 678 [2] V.C. Schreiner, E. Szöcs, A.K. Bhowmik, M.G. Vijver, R.B. Schäfer, Pesticide mixtures in streams of
679 several European countries and the USA, *Science of The Total Environment*, 573 (2016) 680-689.
680 <https://doi.org/10.1016/j.scitotenv.2016.08.163>
- 681 [3] F.J. Benitez, F.J. Real, J.L. Acero, C. Garcia, Photochemical oxidation processes for the elimination
682 of phenyl-urea herbicides in waters, *Journal of hazardous materials*, 138 (2006) 278-287.
683 <https://doi.org/10.1016/j.jhazmat.2006.05.077>
- 684 [4] M.P. Silva, A.P. dos Santos Batista, S.I. Borrely, V.H.O. Silva, A.C.S.C. Teixeira, Photolysis of atrazine
685 in aqueous solution: role of process variables and reactive oxygen species, *Environmental Science
686 and Pollution Research*, 21 (2014) 12135-12142. <https://doi.org/10.1007/s11356-014-2881-0>
- 687 [5] N. Chen, D. Valdes, C. Marlin, P. Ribstein, F. Alliot, E. Aubry, H. Blanchoud, Transfer and
688 degradation of the common pesticide atrazine through the unsaturated zone of the Chalk aquifer
689 (Northern France), *Environmental Pollution*, 255 (2019) 113125.
690 <https://doi.org/10.1016/j.envpol.2019.113125>
- 691 [6] L. Carles, H. Gardon, L. Joseph, J. Sanchís, M. Farré, J. Artigas, Meta-analysis of glyphosate
692 contamination in surface waters and dissipation by biofilms, *Environment International*, 124 (2019)
693 284-293. <https://doi.org/10.1016/j.envint.2018.12.064>
- 694 [7] J. Dollinger, C. Dagès, M. Voltz, Glyphosate sorption to soils and sediments predicted by
695 pedotransfer functions, *Environmental Chemistry Letters*, 13 (2015) 293-307.
696 <https://doi.org/10.1007/s10311-015-0515-5>
- 697 [8] L. Velkoska-Markovska, B. Petanovska-Ilievska, A. Markovski, Application of High Performance
698 Liquid Chromatography to the Analysis of Pesticide Residues in Apple Juice, *Contemporary
699 Agriculture*, 67 (2018) 93-102. doi:10.2478/contagri-2018-0014

700 [9] R.L. Glass, Adsorption of glyphosate by soils and clay minerals, *Journal of Agricultural and Food*
701 *Chemistry*, 35 (1987) 497-500. <https://doi.org/10.1021/jf00076a013>

702 [10] G.-M. Momplaisir, C.G. Rosal, E.M. Heithmar, K.E. Varner, L.A. Riddick, D.F. Bradford, N.G.
703 Tallent-Halsell, Development of a solid phase extraction method for agricultural pesticides in large-
704 volume water samples, *Talanta*, 81 (2010) 1380-1386. <https://doi.org/10.1016/j.talanta.2010.02.038>

705 [11] S. Barrek, C. Cren-Olivé, L. Wiest, R. Baudot, C. Arnaudguilhem, M.-F. Grenier-Loustalot, Multi-
706 residue analysis and ultra-trace quantification of 36 priority substances from the European Water
707 Framework Directive by GC-MS and LC-FLD-MS/MS in surface waters, *Talanta*, 79 (2009) 712-722.
708 <https://doi.org/10.1016/j.talanta.2009.04.058>

709 [12] R. Carabias-Martínez, E. Rodríguez-Gonzalo, E. Herrero-Hernández, F.J. Sánchez-San Román,
710 M.G. Prado Flores, Determination of herbicides and metabolites by solid-phase extraction and liquid
711 chromatography: Evaluation of pollution due to herbicides in surface and groundwaters, *Journal of*
712 *Chromatography A*, 950 (2002) 157-166. [https://doi.org/10.1016/S0021-9673\(01\)01613-2](https://doi.org/10.1016/S0021-9673(01)01613-2)

713 [13] C. Hao, D. Morse, F. Morra, X. Zhao, P. Yang, B. Nunn, Direct aqueous determination of
714 glyphosate and related compounds by liquid chromatography/tandem mass spectrometry using
715 reversed-phase and weak anion-exchange mixed-mode column, *Journal of Chromatography A*, 1218
716 (2011) 5638-5643. <https://doi.org/10.1016/j.chroma.2011.06.070>

717 [14] B. Le Bot, K. Colliaux, D. Pelle, C. Briens, R. Seux, M. Clément, Optimization and performance
718 evaluation of the analysis of glyphosate and AMPA in water by HPLC with fluorescence detection,
719 *Chromatographia*, 56 (2002) 161-164. <https://doi.org/10.1007/BF02493205>

720 [15] T. Arkan, A. Csámpai, I. Molnár-Perl, Alkylsilyl derivatization of glyphosate and
721 aminomethylphosphonic acid followed by gas chromatography mass spectrometry, *Microchemical*
722 *Journal*, 125 (2016) 219-223. <https://doi.org/10.1016/j.microc.2015.11.027>

723 [16] J. Jiang, C.A. Lucy, Determination of glyphosate using off-line ion exchange preconcentration and
724 capillary electrophoresis-laser induced fluorescence detection, *Talanta*, 72 (2007) 113-118.
725 <https://doi.org/10.1016/j.talanta.2006.10.001>

726 [17] C.E. Ramirez, S. Bellmund, P.R. Gardinali, A simple method for routine monitoring of glyphosate
727 and its main metabolite in surface waters using lyophilization and LC-FLD+MS/MS. Case study: canals
728 with influence on Biscayne National Park, *Science of The Total Environment*, 496 (2014) 389-401.
729 <https://doi.org/10.1016/j.scitotenv.2014.06.118>

730 [18] C. Hidalgo, C. Rios, M. Hidalgo, V. Salvadó, J.V. Sancho, F. Hernández, Improved coupled-column
731 liquid chromatographic method for the determination of glyphosate and aminomethylphosphonic
732 acid residues in environmental waters, *Journal of Chromatography A*, 1035 (2004) 153-157.
733 <https://doi.org/10.1016/j.chroma.2004.02.044>

734 [19] J. Patsias, A. Papadopoulou, E. Papadopoulou-Mourkidou, Automated trace level determination
735 of glyphosate and aminomethyl phosphonic acid in water by on-line anion-exchange solid-phase
736 extraction followed by cation-exchange liquid chromatography and post-column derivatization,
737 *Journal of Chromatography A*, 932 (2001) 83-90. [https://doi.org/10.1016/S0021-9673\(01\)01253-5](https://doi.org/10.1016/S0021-9673(01)01253-5)

738 [20] A. Tufail, W.E. Price, M. Mohseni, B.K. Pramanik, F.I. Hai, A critical review of advanced oxidation
739 processes for emerging trace organic contaminant degradation: Mechanisms, factors, degradation
740 products, and effluent toxicity, *Journal of Water Process Engineering*, (2020) 101778.
741 <https://doi.org/10.1016/j.jwpe.2020.101778>

742 [21] J.-L. Shie, C.-H. Lee, C.-S. Chiou, C.-T. Chang, C.-C. Chang, C.-Y. Chang, Photodegradation kinetics
743 of formaldehyde using light sources of UVA, UVC and UVLED in the presence of composed silver
744 titanium oxide photocatalyst, *Journal of Hazardous Materials*, 155 (2008) 164-172.
745 <https://doi.org/10.1016/j.jhazmat.2007.11.043>

746 [22] C. Bertoldi, A.G. Rodrigues, A.N. Fernandes, Removal of endocrine disrupters in water under
747 artificial light: the effect of organic matter, *Journal of Water Process Engineering*, 27 (2019) 126-133.
748 <https://doi.org/10.1016/j.jwpe.2018.11.016>

749 [23] A.M. Díez, M.A. Sanromán, M. Pazos, New approaches on the agrochemicals degradation by UV
750 oxidation processes, *Chemical Engineering Journal*, 376 (2019) 120026.
751 <https://doi.org/10.1016/j.cej.2018.09.187>

752 [24] R.O. Ramos, M.V.C. Albuquerque, W.S. Lopes, J.T. Sousa, V.D. Leite, Degradation of indigo
753 carmine by photo-Fenton, Fenton, H₂O₂/UV-C and direct UV-C: Comparison of pathways, products
754 and kinetics, *Journal of Water Process Engineering*, 37 (2020) 101535.
755 <https://doi.org/10.1016/j.jwpe.2020.101535>

756 [25] E. Blázquez, C. Rodríguez, J. Ródenas, N. Navarro, C. Riquelme, R. Rosell, J. Campbell, J.
757 Crenshaw, J. Segalés, J. Pujols, J. Polo, Evaluation of the effectiveness of the SurePure Turbulator
758 ultraviolet-C irradiation equipment on inactivation of different enveloped and non-enveloped viruses
759 inoculated in commercially collected liquid animal plasma, *PLOS ONE*, 14 (2019) e0212332.
760 [10.1371/journal.pone.0212332](https://doi.org/10.1371/journal.pone.0212332)

761 [26] N. Bustos, A. Cruz-Alcalde, A. Iriel, A. Fernández Cirelli, C. Sans, Sunlight and UVC-254 irradiation
762 induced photodegradation of organophosphorus pesticide dichlorvos in aqueous matrices, *Sci Total*
763 *Environ*, 649 (2019) 592-600. <https://doi.org/10.1016/j.scitotenv.2018.08.254>

764 [27] M. Bavcon Kralj, U. Černigoj, M. Franko, P. Trebše, Comparison of photocatalysis and photolysis
765 of malathion, isomalathion, malaaxon, and commercial malathion—Products and toxicity studies,
766 *Water Research*, 41 (2007) 4504-4514. <https://doi.org/10.1016/j.watres.2007.06.016>

767 [28] P. Somathilake, J.A. Dominic, G. Achari, C.H. Langford, J.-H. Tay, Use of low pressure mercury
768 lamps with H₂O₂ and TiO₂ for treating carbamazepine in drinking water: Batch and continuous flow
769 through experiments, *Journal of Water Process Engineering*, 26 (2018) 230-236.
770 <https://doi.org/10.1016/j.jwpe.2018.10.015>

771 [29] R. Ahmad, Z. Ahmad, A.U. Khan, N.R. Mastoi, M. Aslam, J. Kim, Photocatalytic systems as an
772 advanced environmental remediation: Recent developments, limitations and new avenues for
773 applications, *Journal of Environmental Chemical Engineering*, 4 (2016) 4143-4164.
774 <https://doi.org/10.1016/j.jece.2016.09.009>

775 [30] F. Alberini, M.J.H. Simmons, D.J. Parker, T. Koutchma, Validation of hydrodynamic and microbial
776 inactivation models for UV-C treatment of milk in a swirl-tube 'SurePure Turbulator™', *Journal of*
777 *Food Engineering*, 162 (2015) 63-69. <https://doi.org/10.1016/j.jfoodeng.2015.04.009>

778 [31] T.M. Mac Loughlin, M.L. Peluso, V.C. Aparicio, D.J.G. Marino, Contribution of soluble and
779 particulate-matter fractions to the total glyphosate and AMPA load in water bodies associated with
780 horticulture, *Science of The Total Environment*, 703 (2020) 134717.
781 <https://doi.org/10.1016/j.scitotenv.2019.134717>

782 [32] I. Hanke, H. Singer, J. Hollender, Ultratrace-level determination of glyphosate,
783 aminomethylphosphonic acid and glufosinate in natural waters by solid-phase extraction followed by
784 liquid chromatography–tandem mass spectrometry: performance tuning of derivatization,
785 enrichment and detection, *Analytical and Bioanalytical Chemistry*, 391 (2008) 2265-2276.
786 <https://doi.org/10.1007/s00216-008-2134-5>

787 [33] S. Wang, B. Liu, D. Yuan, J. Ma, A simple method for the determination of glyphosate and
788 aminomethylphosphonic acid in seawater matrix with high performance liquid chromatography and
789 fluorescence detection, *Talanta*, 161 (2016) 700-706. <https://doi.org/10.1016/j.talanta.2016.09.023>

790 [34] T.V. Nedelkoska, G.K.C. Low, High-performance liquid chromatographic determination of
791 glyphosate in water and plant material after pre-column derivatisation with 9-fluorenylmethyl
792 chloroformate, *Analytica Chimica Acta*, 511 (2004) 145-153.
793 <https://doi.org/10.1016/j.aca.2004.01.027>

794 [35] R.J. Vreeken, P. Speksnijder, I. Bobeldijk-Pastorova, T.H.M. Noij, Selective analysis of the
795 herbicides glyphosate and aminomethylphosphonic acid in water by on-line solid-phase extraction–
796 high-performance liquid chromatography–electrospray ionization mass spectrometry, *Journal of*
797 *Chromatography A*, 794 (1998) 187-199. [https://doi.org/10.1016/S0021-9673\(97\)01129-1](https://doi.org/10.1016/S0021-9673(97)01129-1)

798 [36] W.C. Koskinen, L.J. Marek, K.E. Hall, Analysis of glyphosate and aminomethylphosphonic acid in
799 water, plant materials and soil, *Pest Management Science*, 72 (2016) 423-432.
800 <https://doi.org/10.1002/ps.4172>

801 [37] Y.S. Hu, Y.Q. Zhao, B. Sorohan, Removal of glyphosate from aqueous environment by adsorption
802 using water industrial residual, *Desalination*, 271 (2011) 150-156.
803 <https://doi.org/10.1016/j.desal.2010.12.014>

804 [38] I. Freuze, A. Jadas-Hecart, A. Royer, P.-Y. Communal, Influence of complexation phenomena with
805 multivalent cations on the analysis of glyphosate and aminomethyl phosphonic acid in water, *Journal*
806 *of Chromatography A*, 1175 (2007) 197-206. <https://doi.org/10.1016/j.chroma.2007.10.092>
807 [39] M.P. Silva, A.P. dos Santos Batista, S.I. Borrelly, V.H.O. Silva, A.C.S.C. Teixeira, Photolysis of
808 atrazine in aqueous solution: role of process variables and reactive oxygen species.
809 [40] G.V. Buxton, C.L. Greenstock, W.P. Helman, A.B. Ross, Critical Review of rate constants for
810 reactions of hydrated electrons, hydrogen atoms and hydroxyl radicals ($\cdot\text{OH}/\cdot\text{O}^-$ in Aqueous Solution,
811 *Journal of Physical and Chemical Reference Data*, 17 (1988) 513-886. 10.1063/1.555805
812 [41] H. Prosen, L. Zupančič-Kralj, Evaluation of photolysis and hydrolysis of atrazine and its first
813 degradation products in the presence of humic acids, *Environmental Pollution*, 133 (2005) 517-529.
814 <https://doi.org/10.1016/j.envpol.2004.06.015>
815 [42] A.J. Moreira, A.C. Borges, L.F.C. Gouvea, T.C.O. MacLeod, G.P.G. Freschi, The process of atrazine
816 degradation, its mechanism, and the formation of metabolites using UV and UV/MW photolysis,
817 *Journal of Photochemistry and Photobiology A: Chemistry*, 347 (2017) 160-167.
818 <https://doi.org/10.1016/j.jphotochem.2017.07.022>
819 [43] D.W. Kolpin, E.M. Thurman, S.M. Linhart, Finding minimal herbicide concentrations in ground
820 water? Try looking for their degradates, *Science of The Total Environment*, 248 (2000) 115-122.
821 [https://doi.org/10.1016/S0048-9697\(99\)00535-5](https://doi.org/10.1016/S0048-9697(99)00535-5)
822 [44] J.A. Khan, X. He, N.S. Shah, M. Sayed, H.M. Khan, D.D. Dionysiou, Degradation kinetics and
823 mechanism of desethyl-atrazine and desisopropyl-atrazine in water with OH and SO_4^- based-AOPs,
824 *Chemical Engineering Journal*, 325 (2017) 485-494. <https://doi.org/10.1016/j.cej.2017.05.011>
825 [45] W. Li, Y. Zhao, X. Yan, J. Duan, C.P. Saint, S. Beecham, Transformation pathway and toxicity
826 assessment of malathion in aqueous solution during UV photolysis and photocatalysis, *Chemosphere*,
827 234 (2019) 204-214. <https://doi.org/10.1016/j.chemosphere.2019.06.058>
828 [46] S. Navarro, J. Fenoll, N. Vela, E. Ruiz, G. Navarro, Removal of ten pesticides from leaching water
829 at pilot plant scale by photo-Fenton treatment, *Chemical Engineering Journal*, 167 (2011) 42-49.
830 <https://doi.org/10.1016/j.cej.2010.11.105>
831 [47] L. Varanasi, E. Coscarelli, M. Khaksari, L.R. Mazzoleni, D. Minakata.
832 [48] A. Manassero, C. Passalia, A.C. Negro, A.E. Cassano, C.S. Zalazar, Glyphosate degradation in
833 water employing the $\text{H}_2\text{O}_2/\text{UVC}$ process, *Water Research*, 44 (2010) 3875-3882.
834 <https://doi.org/10.1016/j.watres.2010.05.004>
835 [49] J.S. McConnell, R.M. McConnell, Ultraviolet Spectra of Acetic Acid, Glycine, and Glyphosate,
836 *Journal of the Arkansas Academy of Science*, 47 (1993) 73-76.
837 [50] D. Feng, A. Soric, O. Boutin, Treatment technologies and degradation pathways of glyphosate: A
838 critical review, *Science of The Total Environment*, 742 (2020) 140559.
839 <https://doi.org/10.1016/j.scitotenv.2020.140559>
840 [51] K. Lányi, P. Laczay, J. Lehel, Effects of some naturally occurring substances on the
841 photodegradation of herbicide methabenzthiazuron, *Journal of Environmental Chemical Engineering*,
842 4 (2016) 123-129. <https://doi.org/10.1016/j.jece.2015.11.002>
843 [52] B. Balci, M.A. Oturan, N. Oturan, I. Sirés, Decontamination of Aqueous Glyphosate,
844 (Aminomethyl)phosphonic Acid, and Glufosinate Solutions by Electro-Fenton-like Process with Mn^{2+}
845 as the Catalyst, *Journal of Agricultural and Food Chemistry*, 57 (2009) 4888-4894.
846 <https://doi.org/10.1021/jf900876x>
847 [53] J. Liu, J. Fan, T. He, X. Xu, Y. Ai, H. Tang, H. Gu, T. Lu, Y. Liu, G. Liu, The mechanism of aquatic
848 photodegradation of organophosphorus sensitized by humic acid- Fe^{3+} complexes, *Journal of*
849 *Hazardous Materials*, 384 (2020) 121466. <https://doi.org/10.1016/j.jhazmat.2019.121466>
850 [54] J. Jönsson, R. Camm, T. Hall, Removal and degradation of glyphosate in water treatment: a
851 review, *Journal of Water Supply: Research and Technology-Aqua*, 62 (2013) 395-408.
852 10.2166/aqua.2013.080
853 [55] R. Kanissery, B. Gairhe, D. Kadyampakeni, O. Batuman, F. Alferéz, Glyphosate: Its Environmental
854 Persistence and Impact on Crop Health and Nutrition, *Plants*, 8 (2019).
855 <https://doi.org/10.3390/plants8110499>

